PAPER

Reduced chemistries with the Quantemol database (QDB)

Plasma Sci. Technol. **21** (2019) 064006 (14pp) https://doi.org/10.1088/2058-6272/ab00a1

Reduced chemistries with the Quantemol database (QDB)

Adetokunbo AYILARAN[1], Martin HANICINEC[2], Sebastian MOHR[1] and Jonathan TENNYSON[2]

[1] Quantemol Ltd, 320 City Rd, London EC1V 2NZ, United Kingdom
[2] Department of Physics and Astronomy, University College London, London WC1E 6BT, United Kingdom

E-mail: j.tennyson@ucl.ac.uk

Received 3 November 2018, revised 20 January 2019
Accepted for publication 22 January 2019
Published 18 April 2019

Abstract

Typical feed gas mixtures used in technological and other plasmas may give rise to reaction networks involving several hundred reactions. Such chemistries are often too large to be used in full reactor simulations and it is therefore desirable to construct reduced chemistry networks which mimic as closely as possible the behavior of the full chemistry but employ far fewer individual reactions and species. Constructed chemistries are available from the Quantemol database (QDB) and two approaches to constructing reduced chemistry from these chemistries based on (a) physical intuition and (b) sensitivity analysis of dominant reaction pathways, are explored. In doing this it is necessary to consider different pressure and power regimes. Reduced chemistry sets are presented for $CF_4/O_2/N_2/H_2$, for which 396 reactions and 52 species are reduced to 71 reactions and 26 species, and for pure O_2, for which 45 reactions and 10 species are reduced to 34 reactions.

Keywords: plasma chemistries, quantemol database, chemical reactions, chemistry reduction, stoichiometry

(Some figures may appear in colour only in the online journal)

1. Introduction

Low temperature plasmas are characterized by having significant molecular content. These plasmas generally undergo a variety of processes via (a) interactions with electrons which can induce chemical change by, for example, neutral dissociation, (b) chemical reactions between species in the plasma or (c) reactions on the walls of the vessel containing the plasma. Below we describe the gas phase processes for a given feed gas as the plasma chemistry. Using these chemistries as the basis of detailed plasma models is becoming an increasingly important activity scientifically [1, 2]. As a result, databases [3–7] and datasets (for example [8–10]) are being systematically compiled to provide cross sections and rates for processes thought to be important within plasmas. Two of these databases, KIDA [4] and the Quantemol database (QDB) [7], attempt to augment lists of individual processes by providing comprehensive chemistry sets for plasma environments of interest. In the case of KIDA [4], the kinetic database for astrochemistry, these chemistries, which KIDA terms networks, are designed for studies of the interstellar medium. QDB [7], which is the database that concerns us here, is designed for studies of terrestrial plasmas, particularly technological ones used, for example, for silicon etching.

QDB aims not only to provide comprehensive sets of reaction rates and electron collision cross sections, but also offers pre-assembled and validated self-consistent chemistry sets for plasma modelling applications. It is planned that QDB will be augmented with a dynamic chemistry facility which will automatically construct a set of key reactions for a given set of gases and chamber conditions. For this, a method of compiling and reducing complex chemistry is necessary.

Those chemistries available in QDB can contain a relatively modest number of reactions (16 for a pure helium plasma, for example) but the chemistry sets more often contain many hundreds of reactions (for example, 557 for a chemistry based on the use of a CF_4, CHF_3, H_2, Cl_2, O_2, HBr mixture). Performing detailed equipment models for key

plasma processes requires propagating plasma models for complex reactor geometries over many time steps. Doing this for chemistries containing several hundred reactions is at best computationally demanding and in some cases computationally impossible. Indeed, some well-used software packages, such as COMSOL, experience convergence issues which tend to limit the number of reactions that can be used to about 50 [11].

For this reason, it is desirable to design reduced chemistry sets. These are chemistry sets which approximately mimic the behavior of a simulation performed with the full chemistry, while containing a greatly reduced number of species and reactions. Some work in this direction has recently been performed for astrochemical networks appropriate for models of interstellar molecular clouds [12]. However, the low-temperature, near-vacuum conditions found in the interstellar medium gives a set of conditions not found on Earth. Markosyan *et al* [13] presented a tool developed to find dominant reaction pathways which they present as an essential method for chemistry reduction. The tool (called PumpKin) uses the outputs of a zero-dimensional (0D) modeler as inputs where the species concentrations are calculated in steady state and the source term of species production and destruction are calculated from the stoichiometric matrix. This method has strong similarities to the analysis carried out in this work. Here we explore the construction of reduced chemistry sets for terrestrial applications and, in particular, demonstrate that in most cases there will not be a unique reduced chemistry set for all applications but instead it is necessary to design different sets according to the temperature and pressure regime of the plasma being considered.

2. Method

Our aim is to produce reduced chemistry sets with a few tens of reactions starting from complex chemistries containing several hundred reactions. We do this by comparing 0D models for the complete set and various reduced sets. All the 0D models were performed using the πlasma-R 0D modelling code of Kokkoris and co-workers [14, 15]. Monitoring the evolution of the plasma as these parameters are changed involves the use of a 0D modeling code which can comfortably calculate large chemistry sets with the main input being power density and pressure. In particular, modeling using rate constant coefficients kept computation time low. In QDB, these rate constant coefficients, k, are given in the form of the parameters of the Arrhenius equation:

$$k = AT_{\mathrm{e}}{}^{B}\mathrm{e}^{-\frac{C}{T_{\mathrm{e}}}} \tag{1}$$

where T_{e} is the electron temperature, and A, B and C are the constants characterizing the reaction and given by the database. Knowledge of these rates coefficients and of the typical behavior of plasmas under the given conditions can be used to remove reactions and species on the basis of physical intuition.

The use of actual modeling gives a numerical reduction procedure which eliminates conjecture about which reactions to remove and instead uses a combination of stoichiometry and sensitivity analysis to determine the participation of certain species and their reactions within the network that defines the chemistry set [16]. For a given network of reactions, a master chemical kinetics equation [17] can be expressed as:

$$\frac{\mathrm{d}y_i}{\mathrm{d}t} = g(y_i) = \sum_{j=1}^{R} s_{ij}F^j(y_i) \tag{2}$$

where i and j represent the species number and reaction number respectively; R is the total number of reactions in the network; s_{ij} is a stoichiometric coefficient detailing the participation of a species in a given reaction. F_j is the rate of reaction j which depends on y, a list of chemical species that form the system, and their concentrations. As this analysis assumes the plasma is in steady state, the master chemical kinetics equation is characterized by the rate of change of total concentration (if used globally) or specific species concentration (if used locally for a single species). This method also relies on the conservation of the number of elements and the total mass in a given reaction. The rate of change of concentration in the system can be quantified by applying 'changes' to the system. This can be expressed as a perturbation:

$$\frac{\mathrm{d}y_i}{\mathrm{d}t} = g(y_i) + \delta g(y) \tag{3}$$

The perturbation $\delta g(y)$ may represent a reaction missing from the previous calculation of $g(y_i)$, a variation of rate constants (if knowledge of them is uncertain), or any other arbitrary change such as the removal of entire species. Therefore, the identification of dominant pathways that control species concentrations is the primary use of this method whilst sensitivity of these pathways is secondary.

Changing reaction rates or removing reactions/species from the system gives a measure of that change's importance to the system as a whole and manifests itself as a perturbation, $\delta g(y_i)$. The larger the perturbation, the larger the effect on the system. The effect of the perturbations is classified using a coefficient, C_i,

$$C_i = \frac{\delta g(y)}{g(y_i)} \tag{4}$$

It is often the case that, depending on the pressure, removing a reaction or slightly changing its reaction rate will have almost no effect on the system as a whole. This is where the chemistry reduction process takes shape as unimportant reactions with $C_i \sim 0$ are removed, whilst dominant reactions that have a coefficient $|C_i| \geqslant \varepsilon$ are retained, where C_i can typically be as low as 1×10^{-5}.

This method can be considered superior to using physical intuition to decide which reactions and species to neglect as it can be programmed into an algorithm yielding quantitative results which can be used to make informed judgments. This analytical method can be used to define logical steps from a full chemistry set to a reduced one.

In constructing the reduced chemistry set it is necessary to consider a range of physical environments as the reduction is sensitive to the physics that occurs at various pressures and powers and the details of this physics justify the removal of species and reactions from the chemistry set. The most sensitive parameter is pressure, which determines the mean free path of the heavy particles. The reaction rate for heavy particle processes depends on the mean free path, as does the electron temperature, T_e. This means that at high pressures, T_e is reduced and electron–heavy particle collisions favor attachment and dissociation, rather than high energy impact ionization. Furthermore, high pressures enable neutral–neutral collisions to occur on length scales comparable to, or less than, the reactor vessel dimensions. Very low pressures reduce the chances of neutral–neutral collisions and most heavy particle collisions are therefore charge-exchange and neutralization. So different reactions dominate in different pressure regimes and these regimes can be associated with specific applications. We therefore divide our considerations into the following pressure regimes and example applications:

Very low pressure: 1–30 mTorr; application: ion bombardment etching;

Low pressure: 30–100 mTorr; application: ion etching with some neutral assistance;

Medium pressure: 100–500 mTorr; application: some ion etching with neutral coverage;

High pressure: 500–1000 mTorr, application: neutral deposition.

The other parameter that needs to be considered is power. Variation of power has a minimal effect on T_e but mainly controls the electron density. Varying the power controls dissociation of the plasma species and the density of charged species in the plasma. A plasma with a high power input or high power density is likely to be very fractionated and electropositive. This is because as the power is raised, the electron density is also raised. The increase in electron density leads to a higher degree of dissociation, i.e. a larger number of atomic species to molecular species. As negative ions are created by dissociative attachment of molecular species, the density of negative ions decreases as the proportion of atomic species increases.

3. Examples of practical reduced chemistry

As a working example, we use the chemistry arising from a feed gas mixture $CF_4/O_2/N_2/H_2$. This gas mixture, with varying initial plasma conditions, is used in remote plasma chemical etching, direct plasma etching with CF_4/O_2 of poly-Si and SiO_2 with additions of N_2 and H_2 depending on the surface of the substrate and dry reactive ion etching in silicon via (TSV) cleaning [18–20].

We carried out 0D chemistry modelling based upon the reactor and process settings used in a previous 2D investigation; these are given in table 1.

The chemistry set for $CF_4/O_2/N_2/H_2$ available from QDB contains 396 reactions, data on which were taken from references [21–29], involving 52 species; this chemistry forms our base set.

Table 1. Details of parameters used in our model of a microwave reactor.

Property	Value
Reactor	Microwave
Power range (W)	0–2000
Pressure range (mTorr)	1–1000
Gas mixture	$CF_4/O_2/N_2/H_2$
Percentage of gas (%)	0.1/85/14.15/0.75
Total gas flow (SCCM)	3780

3.1. Physical intuition

Figure 1 illustrates the effect of increasing the pressure and/or density of the feed gas. In general, as the pressure increases less of the gas is consumed in electron impact collisions and gas phase recombination reactions happen more frequently. The discharge becomes more electronegative and this is illustrated by the increase in negative charge density. The electron temperature is notably lowered as the pressure increases due to the smaller mean free path. There is a point at medium pressure where atomic positive ions are at their highest densities.

Figure 2 shows the behavior of the plasma as a function of initial power. As expected, we observe an increase in electron density and atomic species, most notably atomic positive ions. There is seen to be some noticeable decrease in NH_x species and this can be attributed to combined mechanisms of dissociation and the fact that the H^- ion density gradually decreases, which follows on from the lowered electronegativity of the discharge. The increase in dissociation is followed by a visible decrease in feed gas and increase in atomic/feed gas ratio. Because the production of heavy neutral ground state species generally depends on the recombination of radicals, their densities also increase before plateauing.

Initial reduced chemistry sets were constructed using physical intuition for a pressure of 10 mTorr and the power of 1000 W. Physical intuition can allow one to make sweeping assumptions and reduce chemistry based upon the physics of the discharge. The low pressure means that neutral–neutral collisions are rare due to mean free paths which are greater than the system size. There are also effectively no negative heavy ions due to the high degree of dissociation. Furthermore, if an etching process is required, 10 mTorr partially ensures the anisotropy of energetic ions—although this is generally in combination with high voltage sheaths.

Although some of the percentage changes may look alarming (up to 100% is actually acceptable as doubling/halving of densities is within an order of magnitude), densities within the same order of magnitude are generally acceptable. For species with very low densities predominantly, it is not uncommon to experience large changes in densities during studies as there is general uncertainty in

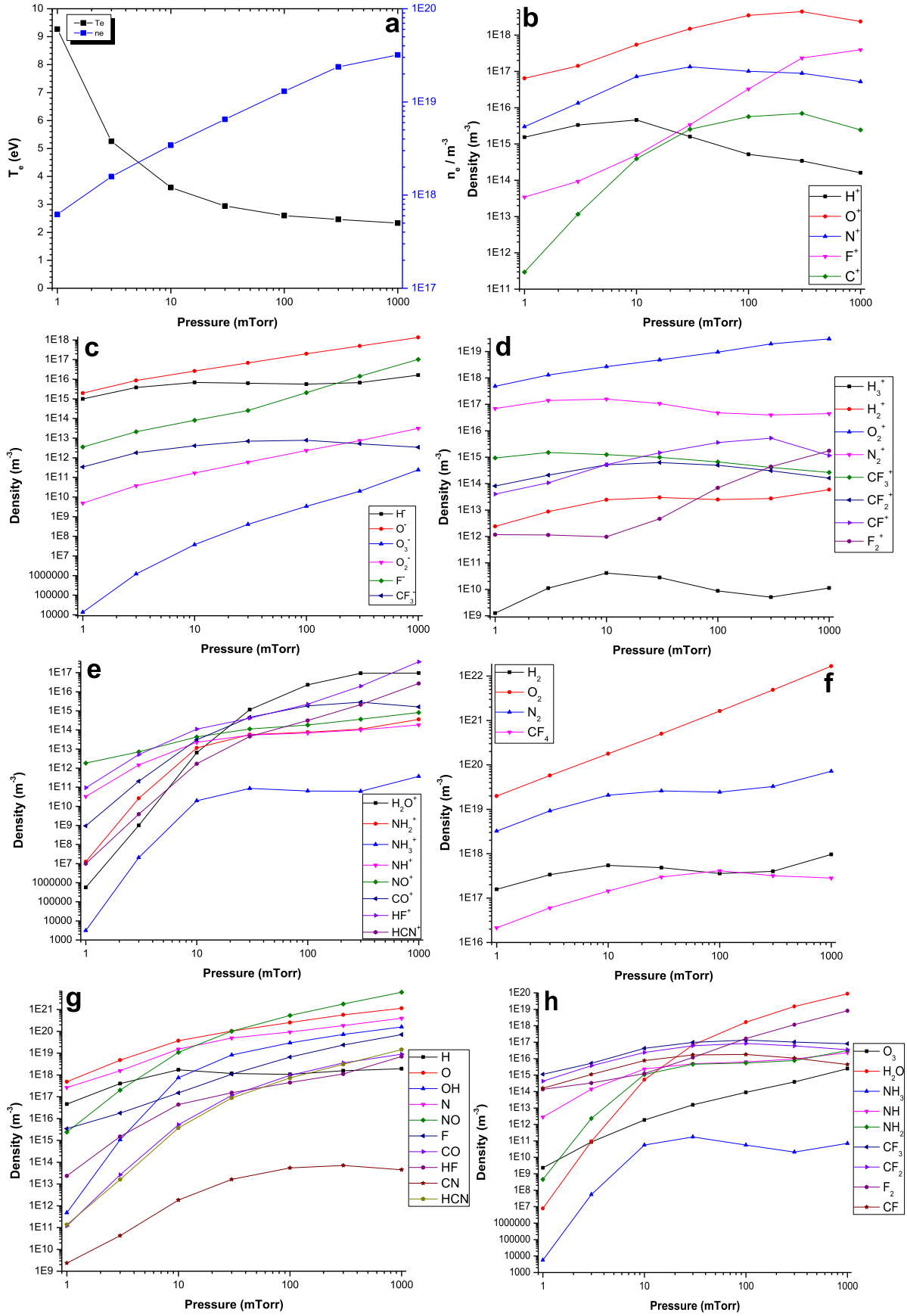

Figure 1. Concentrations of species in the plasma as a function of initial pressure for a power of 1000 W. (a) electron density and temperature, (b) positive atomic ion density, (c) negative ion density, (d) heavy positive ion density, (e) ionized molecule densities, (f) neutral molecule densities, (g) neutral radical densities, and (h) feed gas densities.

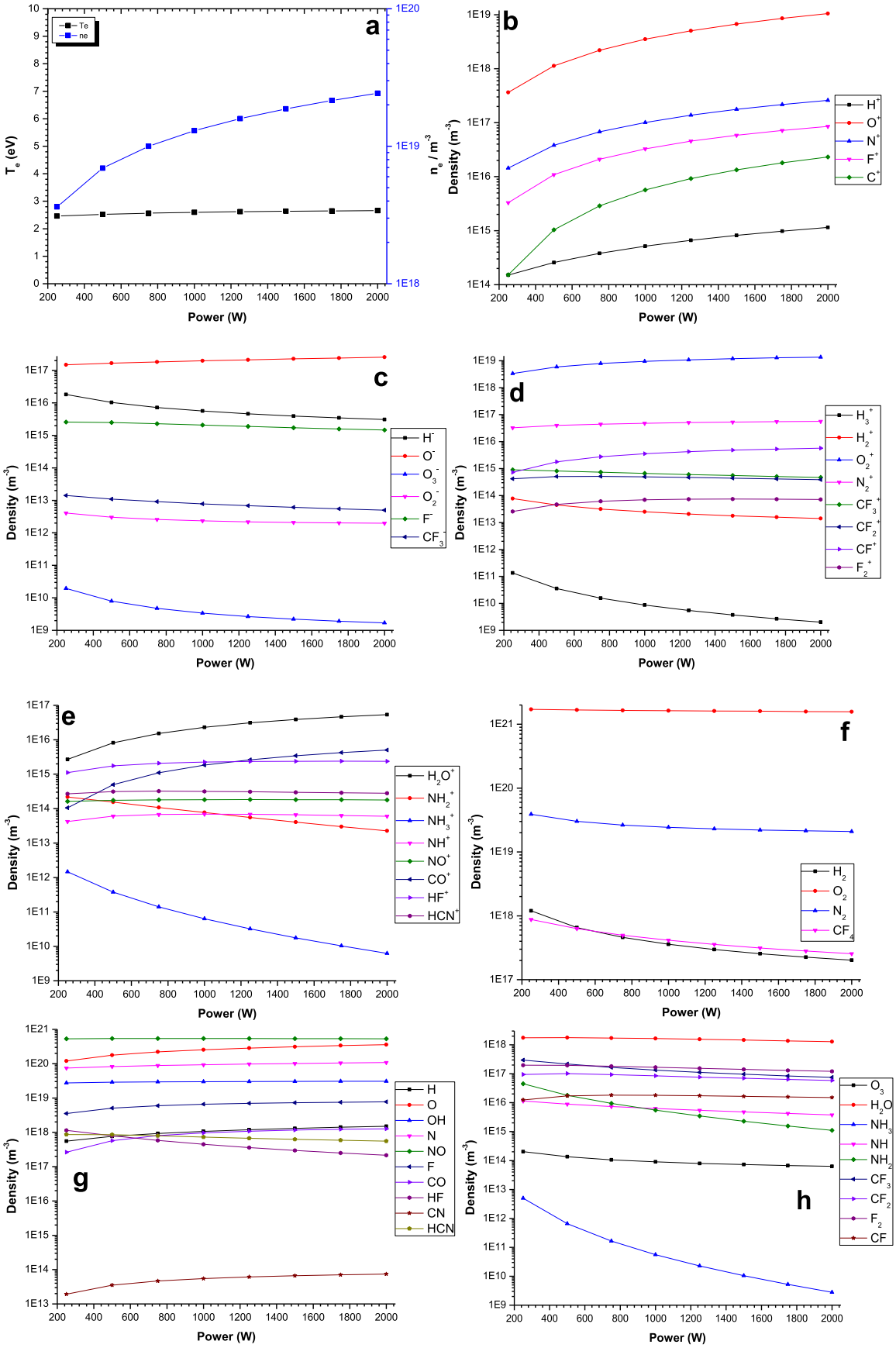

Figure 2. Concentrations of species in the plasma as a function of power at a pressure of 10 mTorr. (a) electron density and temperature, (b) positive atomic ion density, (c) negative ion density, (d) heavy positive ion density, (e) ionized molecule densities, (f) neutral molecule densities, (g) neutral radical densities, and (h) feed gas densities.

Table 2. Densities and electron energies for the full and reduced set using physical intuition.

Species	Reduced set (m^{-3})	Full set (m^{-3})	Percentage change
H_2	1.04E + 18 m^{-3}	5.43E + 17 m^{-3}	91.52%
H	1.54E + 18 m^{-3}	1.72E + 18 m^{-3}	10.46%
H^+	2.45E + 15 m^{-3}	4.59E + 15 m^{-3}	46.62%
O_2	1.82E + 20 m^{-3}	1.78E + 20 m^{-3}	2.25%
O^-	2.72E + 16 m^{-3}	2.64E + 16 m^{-3}	3.03%
O	4.09E + 19 m^{-3}	3.70E + 19 m^{-3}	10.54%
O_2^+	2.67E + 18 m^{-3}	2.67E + 18 m^{-3}	0%
O^+	5.65E + 17 m^{-3}	5.45E + 17 m^{-3}	3.67%
N_2	3.01E + 19 m^{-3}	2.08E + 19 m^{-3}	30.9%
N	7.63E + 18 m^{-3}	1.54E + 19 m^{-3}	50.45%
N_2^+	2.20E + 17 m^{-3}	1.57E + 17 m^{-3}	40.13%
N^+	3.85E + 16 m^{-3}	7.20E + 16 m^{-3}	46.53%
CF_4	1.93E + 17 m^{-3}	1.45E + 17 m^{-3}	33.1%
F	9.67E + 16 m^{-3}	1.50E + 17 m^{-3}	35.53%
CF_3	1.27E + 16 m^{-3}	4.29E + 16 m^{-3}	70.4%
CF_2	1.82E + 16 m^{-3}	2.36E + 16 m^{-3}	22.88%
CF_3^+	1.31E + 15 m^{-3}	1.26E + 15 m^{-3}	3.97%
F^+	2.98E + 14 m^{-3}	4.89E + 14 m^{-3}	39.06%
CF_2^+	3.48E + 14 m^{-3}	5.12E + 14 m^{-3}	32.03%
CF^+	5.66E + 14 m^{-3}	5.25E + 14 m^{-3}	7.81%
CF	1.07E + 16 m^{-3}	7.73E + 15 m^{-3}	38.42%
T_e	3.560 99 eV	3.603 42 eV	1.18%
n_e	3.47E + 18 m^{-3}	3.42E + 18 m^{-3}	1.46%

their measurement, especially when measured experimentally. The biggest changes are seen from the H_2 density and this can be attributed to its dissociation being due to H formation and not other pathways such as H_2^+ and H_3^+. The removal of these species means that the main loss process of H_2 is due to its dissociation. The concentration of molecular hydrogen is very small compared to the other feed gases and its density is of the same order as the electron density, hence, the change in density is reasonable even though ionization usually does not change the neutral densities significantly. CF_3 similarly has a noticeable change due to the removal of pathways that include the recombination or neutralization of CF_3^+ and F^+, as these species exist in very low concentrations. It is important to be wary of removing such possible intermediate species. In this case, the bulk of the CF_3 density comes from the electron impact dissociation of CF_4, so other pathways that include F^+ and $CF_3{}^+$ can be neglected. However, for other species its low density may be because its destruction pathway sustains the density of another species. This can be difficult to see intuitively unless seen beforehand or by using numerical sensitivity analysis.

Table 2 shows results obtained using physical intuition. Using this method the 396 reactions were reduced to 50 key reactions and 21 species. Many of the rates are dominated by the electron density which, as can be seen, does not change significantly. This reduction was done in several steps:

- Choosing a pressure range to examine the participation of certain types of collisions
  Neutral–neutral collisions
  Charge-exchange collisions
  Charge-neutralization collisions
  Electron impact ionization collisions
  Electron impact dissociation collisions
- Choosing a power range to examine the dissociation of the plasma
  High power is highly dissociative due to large electron densities and therefore high ionization rates
  Low power is weakly dissociated due to lower electron densities and therefore low ionization rates

The following species were removed from the chemistry along with all the reactions involving them. Anions O_3^-, O_2^- and CF_3^- were removed as they are heavy negative ions and dissociative processes dominate the plasma; C and C^+ were removed as C and C^+ densities remain low due to consecutive recombination and deposition only occurring far from the main power absorption region. H_2O, H_2O^+, CO, CO^+, CN, HCN, HCN^+, HF and HF^+ were removed as the ground states are the products of neutral gas-phase collisions which occur very infrequently at a pressure of 10 mTorr and the ionized species are created by charge-exchange of the ground state.

Other species suspected of being of reduced importance included H^-, F^- O_3, NH_2, NH_2^+, H_2^+, H_3^+, NO, NO^+, F_2^+ and F_2. These species were removed and new reduced chemistry was again compared with the full set at 10 mTorr. Further species were then removed starting with the anions H^- and F^- as their concentration was more than three orders of magnitude lower than the electron density. At this power and pressure, negative charge density is dominated by electrons and only O^- ions are noticeable. O_3 was removed as its dissociation processes are most likely to be dominant and its density becomes negligible below 100 mTorr. NH, NH^+, NH_2, NH_2^+, NH_3 and NH_3^+ were all removed due to the removal of H^- meaning there was no production of NH which is necessary for heavier NH_x formation. H_2^+ and H_3^+ were removed as the high degree of dissociation results in a very high density of H atoms; if H_2^+ is removed, H_3^+ must also be removed as H_2^+ is the intermediate to its formation. F_2 and F_2^+ were removed as their production appears to increase with pressure and is therefore very low at the pressure under consideration.

Regardless of the physical insight, one must be able to demonstrate the validity of removing certain species. Thus, for example, Yang *et al* [30] stresses the importance of including H^- even at low pressures approaching 7.5 mTorr in a pure H_2 discharge in order to correctly determine the electron density and pressure. The removal of the NH_x species from our chemistry means that an important loss process for H^+ ($N + H^+ \rightarrow NH + e$) is no longer prevalent. As a result, the H^- density before removal of NH is $6.85 \times 10^{15}\ m^{-3}$ which is reduced to $5.71 \times 10^{15}\ m^{-3}$ after removal of NH. Losses processes of H^- are still overwhelmingly large due to charge neutralization with O_x^+, N_x^+ and H_x^+ species. Furthermore, removal of H^- from the plasma did not affect the species of O_x^+, N_x^+ and H_x^+. So without it being an important intermediary step and not being particularly important in

Table 3. Reactions used to construct pure oxygen chemistry in QDB.

Reaction number	Mechanism	Rate coefficient (m^{-6} s^{-1})
1	$e + O_2 \rightarrow O^* + O + e$	$5.08 \times 10^{-17} T_e^{1.18} e^{-\frac{8.96}{T_e}}$
2	$e + O_2 \rightarrow O_2^* + e$	$2.40 \times 10^{-14} T_e^{0.20} e^{-\frac{7.481}{T_e}}$
3	$e + O_2 \rightarrow O^- + O$	$6.74 \times 10^{-16} T_e^{-1.02} e^{-\frac{5.78}{T_e}}$
4	$e + O_2 \rightarrow O + O + e$	$1.75 \times 10^{-14} T_e^{-1.28} e^{-\frac{7.38}{T_e}}$
5	$e + O_2 \rightarrow O_2^+ + e + e$	$7.08 \times 10^{-15} T_e^{0.76} e^{-\frac{13.81}{T_e}}$
6	$e + O_2^* \rightarrow O_2^+ + e + e$	$1.3 \times 10^{-15} T_e^{1.1} e^{-\frac{11.1}{T_e}}$
7	$e + O_2 \rightarrow O^+ + O + e + e$	$9.92 \times 10^{-16} T_e^{1.101} e^{-\frac{20.30}{T_e}}$
8	$e + O_2^+ \rightarrow O + O$	$1.53 \times 10^{-14} T_e^{-0.51} e^{-\frac{0.013}{T_e}}$
9	$e + O \rightarrow O^+ + e + e$	$4.82 \times 10^{-15} T_e^{0.74} e^{-\frac{13.11}{T_e}}$
10	$e + O^- \rightarrow O + e + e$	$1.95 \times 10^{-18} T_e^{-0.5} e^{-\frac{3.4}{T_e}}$
11	$e + O^* \rightarrow O + e$	$5.82 \times 10^{-15} T_e^{-0.20} e^{-\frac{1.08}{T_e}}$
12	$e + O^* \rightarrow O^+ + e + e$	$1.56 \times 10^{-14} T_e^{0.29} e^{-\frac{13.30}{T_e}}$
13	$e + O_3 \rightarrow O_2 + O^-$	$1.87 \times 10^{-15} T_e^{-1.30} e^{-\frac{0.97}{T_e}}$
14	$e + O_3 \rightarrow O_2^- + O$	$8.81 \times 10^{-16} T_e^{-1.42} e^{-\frac{1.064}{T_e}}$
15	$O + O^- \rightarrow O_2 + e$	$3 \times 10^{-16} T_e^{-0.5}$
16	$O^- + O_2^+ \rightarrow O_2 + O$	1×10^{-13}
17	$O^- + O^+ \rightarrow O + O$	1×10^{-13}
18	$O_2 + O^- \rightarrow O_3 + e$	5×10^{-21}
19	$O^- + O^+ \rightarrow O + O^*$	2×10^{-13}
20	$O^* + O_3 \rightarrow O_2 + O_2$	1.2×10^{-16}
21	$O_2^* + O_2 \rightarrow O + O_3$	2.95×10^{-27}
22	$O^- + O_3 \rightarrow e + O_2 + O_2$	$3.01 \times 10^{-16} T_g^{0.5} e^{-\frac{0}{T_e}}$
23	$O + O_3^- \rightarrow O_2 + O_2^-$	3.2×10^{-16}
24	$O^- + O_2^* \rightarrow O_3 + e$	3×10^{-16}
25	$O_2^+ + O_2^- \rightarrow O_2 + O_2^*$	2×10^{-13}
26	$O + O_3 \rightarrow O_2 + O_2$	8×10^{-18}
27	$O^+ + O_3 \rightarrow O_2 + O_2^+$	1×10^{-16}
28	$O^- + O_2 \rightarrow e + O_3$	5×10^{-21}
29	$O_2^+ + O_3^- \rightarrow O_2^* + O_3$	$2 \times 10^{-13} T_g^{-0.5} e^{-\frac{0}{T_e}}$
30	$O^+ + O_3 \rightarrow O_2 + O_2^+$	1×10^{-16}
31	$O^- + O_3 \rightarrow O_2 + O_2^-$	$1.02 \times 10^{-17} T_g^{0.5} e^{-\frac{0}{T_e}}$
32	$O_2^+ + O_3^- \rightarrow O + O + O_3$	1×10^{-13}
33	$O_2^+ + O_2^- \rightarrow O + O + O_2$	1×10^{-13}
34	$O + O_3^- \rightarrow O_2 + O_2^-$	3.2×10^{-16}
35	$O^- + O_2^+ \rightarrow O + O + O$	$2 \times 10^{-13} T_g^{-0.5} e^{-\frac{0}{T_e}}$
36	$O_2^+ + O_3^- \rightarrow O_2 + O_3$	1×10^{-13}
37	$O^+ + O_3^- \rightarrow O + O_3$	1×10^{-13}
38	$O_2^+ + O_2^- \rightarrow O_2 + O_2$	1×10^{-13}
39	$O^+ + O_2^- \rightarrow O + O_2$	1×10^{-13}
40	$O + O_2^- \rightarrow O_3 + e$	1.5×10^{-16}
41	$e + O_2 \rightarrow O_2 + e$	$3.93 \times 10^{-14} T_e^{0.63} e^{\frac{0.019}{T_e}}$
42	$e + O \rightarrow O + e$	$6.47 \times 10^{-14} T_e^{0.33} e^{-\frac{0.47}{T_e}}$
43	$O + O_2^+ \rightarrow O_2 + O^+$	2×10^{-17}
44	$O + O^+ \rightarrow O + O^+$	1×10^{-15}
45	$O_2^+ + O_2 \rightarrow O_2^+ + O_2$	1×10^{-15}

correctly estimating the plasma parameters of electron density and temperature, H^- was removed.

3.2. Numerical stoichiometric analysis

3.2.1. Oxygen chemistry. A simpler example involves an O_2 chemistry at high pressure (600 Torr). The reaction set includes 45 gas phase reactions and is reduced to 34 reactions based upon numerical reduction. Due to the smaller size of the chemistry, global analysis was applied and the entire chemistry set was studied in order to eliminate unimportant reaction pathways. This particular chemistry was chosen not just for its smaller size, but because it contains 'exotic' species in the form of O_3, O_2^- and O_3^-, as well as metastable states, which are important intermediaries whilst their concentrations are very much dependent on pressure. The chemistry extracted from QDB is shown in table 3; data for

Table 4. Changes in electron temperature and density, and species concentration for the reduction performed at 600 Torr.

Species	Reduced (m^{-3})	Full (m^{-3})	Percentage change
O_2	9.55E+22	9.55E+22	0%
O^*	7.75E+18	8.36E+18	7.29%
O	8.50E+21	8.51E+21	0.12%
$O_2{}^*$	1.15E+25	1.15E+25	0%
O	9.22E+17	9.22E+17	0%
O_2	1.30E+21	1.30E21	0%
O	1.71E+19	1.21E+19	41.32%
O_3	2.79E+21	2.79E+21	0%
O_2	1.68E+18	1.68E18	0%
O_3	1.16E+16	7.76%	
T_e	1.53 eV	1.53 eV	0%
n_e	1.31E+21	1.31E+21	0%

individual processes were taken from Brian [31], Itikawa [32] and Kossyi *et al* [33].

For this analysis, both symmetric charge exchange reactions and elastic collisions were omitted due to them contributing to matrix sparsity, as well as them being crucial to discharge energy balance in an ideal modelling investigation.

Table 4 illustrates the changes in species concentration before and after reduction at 600 Torr. Being able to reduce a potentially complex set by about 25% without deviating greatly from the physics of the discharge is a significant advantage for 2D and 3D modelling. Table 4 suggests that the reduction eliminates unimportant pathways but maintains the overall behavior of the discharge.

Because this reduction was performed for a very high pressure, the same reduction is unlikely to work at lower pressures. To test this, the pressure was varied and species densities between the reduced and full sets were compared. Figure 3 shows the results of numerical tests with pressures between 10 mTorr and 1000 Torr.

In essence, species whose participation in important reaction pathways is uncertain show a divergence in results between the reduced and full sets as the pressure is varied. This is illustrated particularly in the O^* comparison where there is a noticeable deviation in densities in the middle of the parameter space. It can also be seen that for the heavier species (O_3 and O_3^-), there is again noticeable deviation in the middle of the parameter space. This particular region represents a medium/high pressure region where there are many competing physical processes. It therefore becomes more uncertain which reaction pathways are dominant in these regions. Therefore, reduction via analysis must be undertaken again at those pressures. Since chemistry reduction must preserve the physical behavior of the plasma, the major plasma parameters such as electron density n_e and electron temperature T_e must not deviate significantly. It can be seen from the top panels in figure 3 that the values for the reduced and full chemistry overlap almost perfectly with very minor difference in the middle of the pressure parameter space for T_e.

Table 5. Reaction coefficients for the O_2 chemistry set given in table 3 used in the high pressure reduction.

	Coefficient C_i
1	3.0449E-04
2	7.2378E-05
3	~0
4	3.1437E-01
5	1.4749E-03
6	6.7164E-01
7	1.3739E-05
8	2.7901E-05
9	3.7209E-04
10	~0
11	~0
12	3.1006E-07
13	8.5243E-02
14	1.8048E-02
15	~0
16	2.3749E-03
17	2.2873E-05
18	~0
19	~0
20	1.1524E-04
21	~0
22	8.1073E-04
23	~0
24	1.3040E-01
25	1.7875E-02
26	7.8223E-03
27	1.3930E-04
28	~0
29	5.5463E-06
30	1.3930E-04
31	~0
32	7.4561E-05
33	2.2190E-03
34	~0
35	2.0690E-04
36	2.7901E-05
37	2.7115E-07
38	8.9597E-03
39	4.1802E-05
40	3.2198E-05

Table 5 gives the reaction coefficients for the O_2 chemistry set determined by the sensitivity analysis. In the global system, the most important reactions (to within $\frac{1}{1000}$) that control species concentrations are illustrated in figure 4.

The coefficient of zero for reaction 3, dissociative electron attachment (DEA) of O_2 via $e + O_2 \rightarrow O + O^-$, is misleading. This reaction pathway is the primary source of O^- ions, yet either its global presence is insensitive, or the method wrongly considers it negligible to the system as a whole. Local sensitivity of the O^- ion concentration, however, identifies this pathway as important to the concentration of O^-, see figure 5.

What the method does not recognize, however, is that the pathway of $e + O_3 \rightarrow O_2 + O^-$ depends directly on the

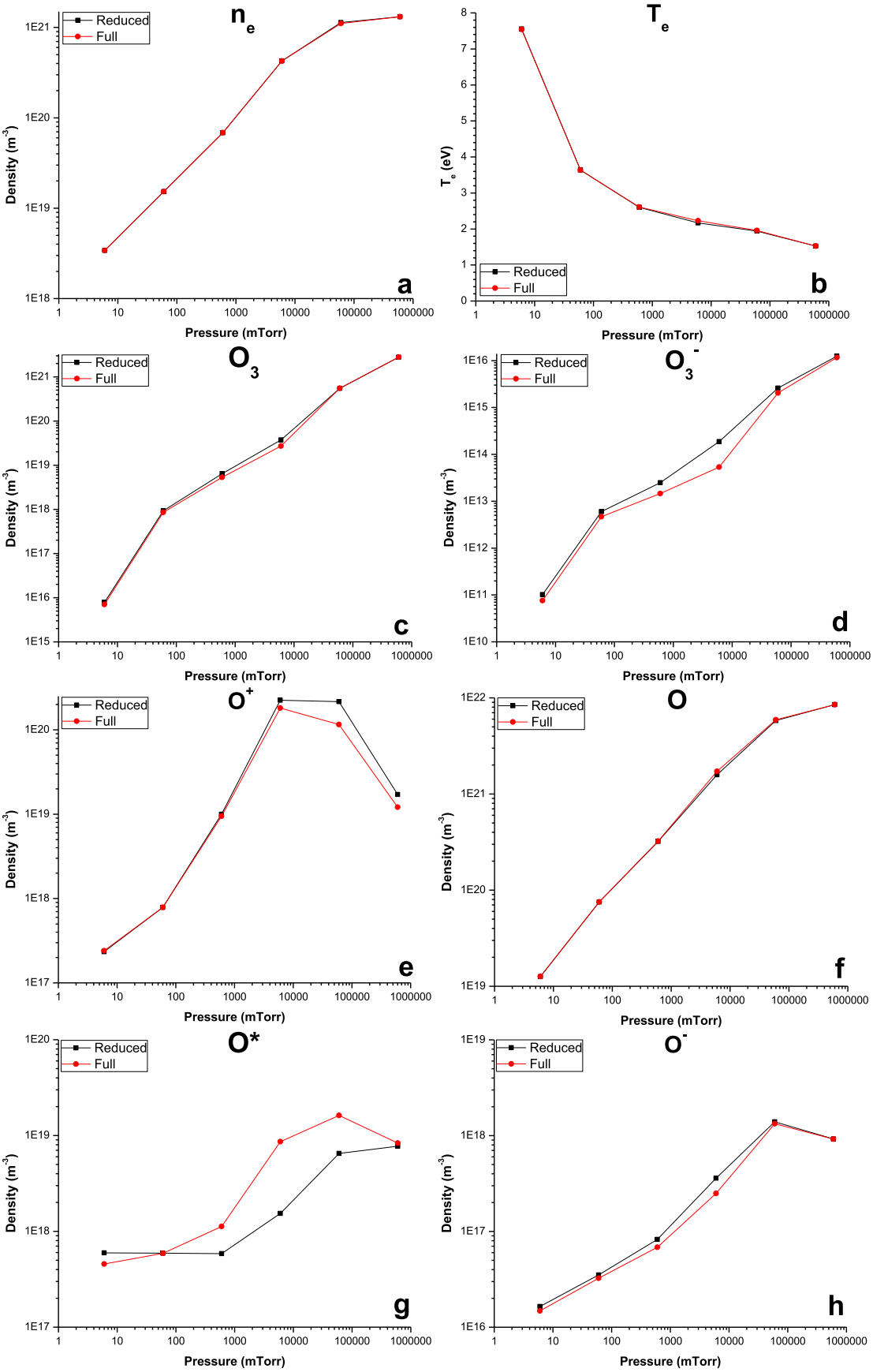

Figure 3. Comparison of various species for the full chemistry and a reduced chemistry generated at high pressure: (a) electron density, (b) electron temperature, (c) O_3 density, (d) O_3^- density, (e) O^+ density, (f) O density, (g) O^* density, and (h) O^- density.

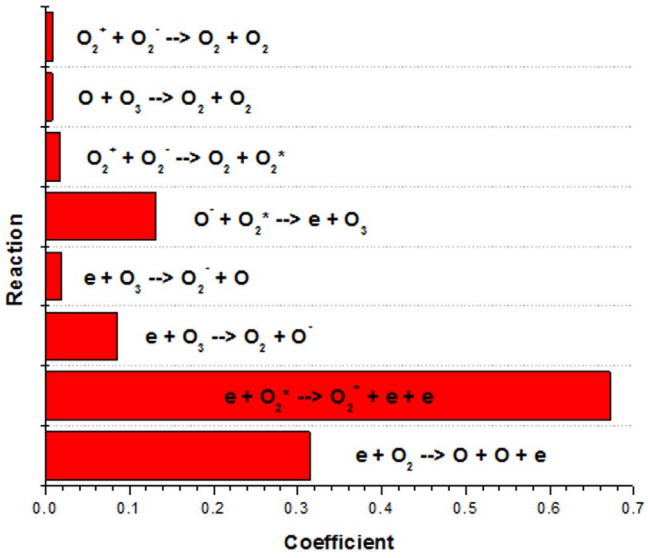

Figure 4. Coefficients of important pathways within the O_2 global system.

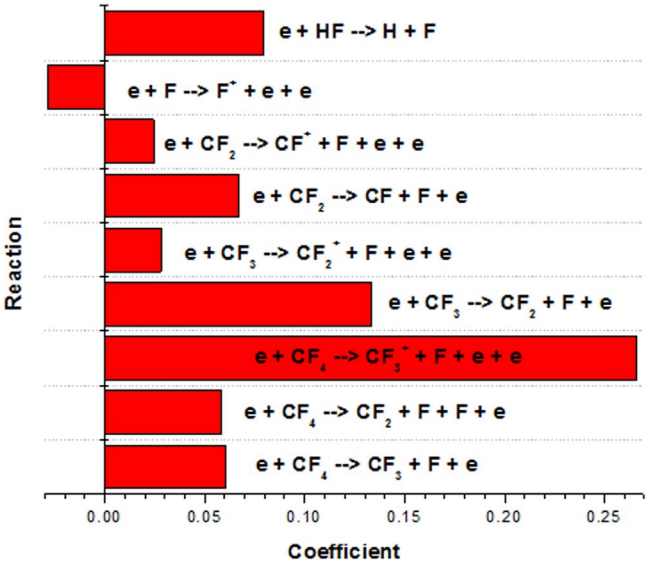

Figure 6. Dominant pathways of F production and loss in the low pressure $CF_4/O_2/N_2/H_2$ chemistry.

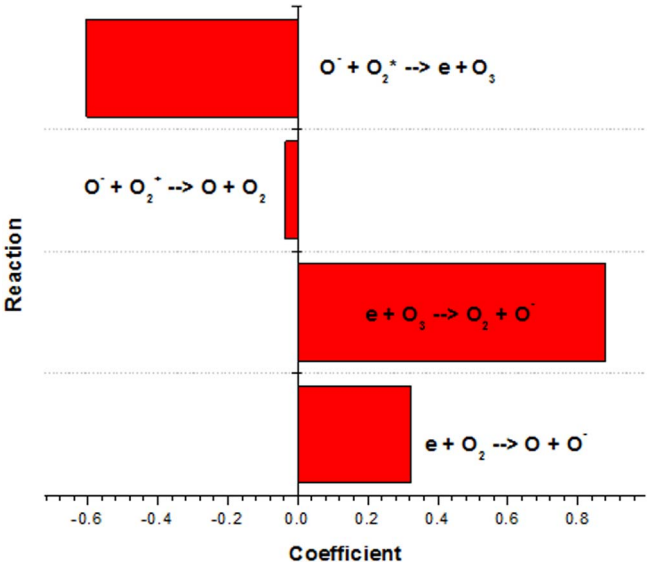

Figure 5. Coefficients of dominant pathways within the O^- local system.

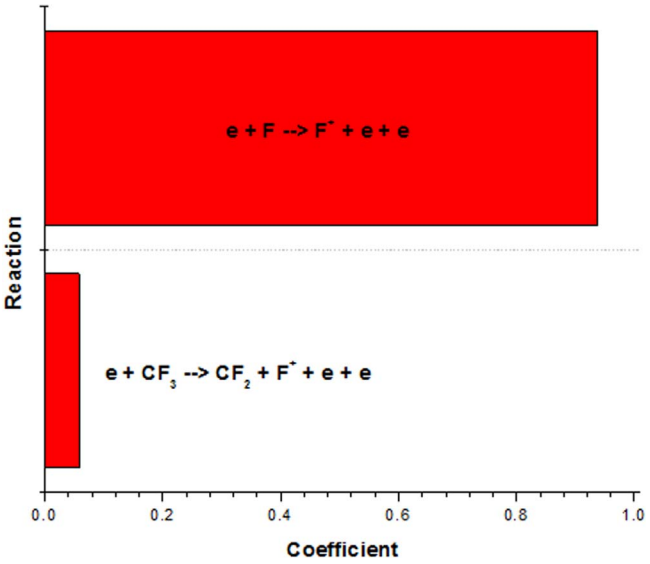

Figure 7. Dominant pathways for F^+ production and loss in the $CF_4/O_2/N_2/H_2$ chemistry.

production of O^- as the formation of O_3 in the system is dominated by associative ionization: $O_2 + O^- \rightarrow O_3 + e$.

3.2.2. $CF_4/O_2/N_2/H_2$ chemistry. Due to the size of the $CF_4/O_2/N_2/H_2$ chemistry and the fact that it was reduced by hand, three local systems of important species were created; F, F^+ and O. This analysis was attempted by modelling the discharge at 10 mTorr. Using reduction via numerical sensitivity analysis, the reaction set was reduced from 396 to 71 reactions, and the species involved halved from 52 to 26.

Again in concordance with the plasma conditions, the main loss process of atomic F is its subsequent ionization mechanism. Sources for F include the electron impact dissociation of CF_x species, see figure 6.

Figure 7 shows the important mechanisms for gas-phase F^+ production and loss. The fact that gas phase loss processes were insensitive suggests that the main loss process for F^+ involves recombination on nearby surfaces via the Bohm process. This is actually in accordance with the 10 mTorr plasma conditions and helps to confirm our numerical analysis in chemistry reduction.

Figure 8 shows that the main source of atomic oxygen is from the dissociation of the O_2 feed gas whilst the main loss process is the resultant ionization of the atom. Note that the dissociation of OH is eventually ignored in the final reduction

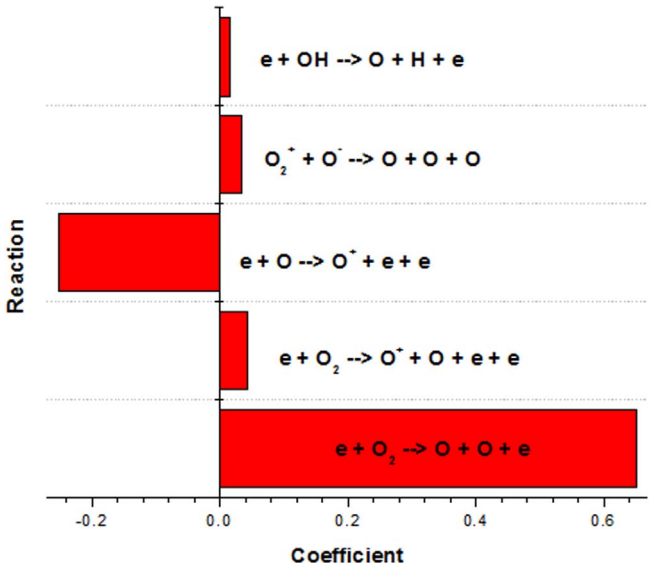

Figure 8. Dominant pathways of O production and loss.

due to the OH density being low and its dissociation not being an important intermediate step for the rest of the discharge.

Figure 9 shows the variation of T_e, n_e and the concentration of F and O with pressure as predicted with the full and reduced (low pressure) chemistry. It can be seen that the plasma parameters agree very closely in the low pressure region. Divergence begins at high pressure. The two local systems used for reduction were F and O. F being the main etchant in this chemistry means that the uncertainty regarding its pathways is very low and the main sources of its production are prevalent at all pressures. Divergence of O on the other hand can be seen as the pressure is increased to where the discharge behavior begins to exhibit more varied processes.

Figure 10 shows some species evolutions whose local systems were not investigated and it can be seen that divergence from the low pressure densities is very noticeable —especially in the case of CF_3^+—which is an example of perturbation of another local system.

Close agreement is expected from 1 mTorr to 30 mTorr as sensitivity analysis at 10 mTorr is based on a very low pressure regime. It can be seen, however, that using the same reduced set for higher pressure begins to yield diverged results which do not really agree with each other and this is expected as the plasma becomes more collision dominated and heavy-particle gas phase collisions (some of which were removed) become a lot more dominant.

Table 6 shows the densities and electron parameters for the full and reduced $CF_4/O_2/N_2/H_2$ chemistry obtained using our numerical sensitivity procedure. The density changes for CF_2^+ and CF_3^+ are caused by not taking into account other local systems. A way around this would be global analysis, but the side effect of this is having certain important reaction pathways appear insensitive as the densities of these ions are about three orders of magnitude smaller than the electron density. These larger relative changes are not expected to influence the plasma as a whole.

Table 6. Densities and electron energies for the full and reduced $CF_4/O_2/N_2/H_2$ chemistry obtained using numerical sensitivity analysis.

Species	Reduced set	Full set	Percentage change
H_2	6.04E + 17 m^{-3}	5.74E + 17 m^{-3}	5.27
H	2.34E + 18 m^{-3}	2.21E + 18 m^{-3}	5.91
H^+	5.72E + 15 m^{-3}	5.56E + 15 m^{-3}	2.79
H^-	6.25E + 15 m^{-3}	4.04E + 15 m^{-3}	54.53
O_2	1.81E + 20 m^{-3}	1.78E + 20 m^{-3}	1.72
O^-	4.09E + 16 m^{-3}	2.65E + 16 m^{-3}	54.34
O	4.13E + 19 m^{-3}	3.77E + 19 m^{-3}	9.46
O_2^+	2.64E + 18 m^{-3}	2.65E + 18 m^{-3}	0.27
O^+	5.91E + 17 m^{-3}	5.49E + 17 m^{-3}	7.65
N_2	3.00E + 19 m^{-3}	2.08E + 19 m^{-3}	44.25
N	7.66E + 18 m^{-3}	1.66E + 19 m^{-3}	53.81
N_2^+	2.14E + 17 m^{-3}	1.58E + 17 m^{-3}	0.01
N^+	3.19E + 16 m^{-3}	7.75E + 16 m^{-3}	58.82
CF_4	1.35E + 17 m^{-3}	1.35 + 17 m^{-3}	0.51
F	1.08E + 16 m^{-3}	1.56E + 17 m^{-3}	30.49
F^-	9.26E + 13 m^{-3}	8.31E + 13 m^{-3}	11.43
CF_3	6.05E + 16 m^{-3}	4.87E + 16 m^{-3}	24.31
CF_2	2.31E + 16 m^{-3}	2.45E + 16 m^{-3}	14.05
CF_3^+	4.35E + 15 m^{-3}	1.23E + 15 m^{-3}	252.58
F^+	3.51E + 14 m^{-3}	5.09E + 14 m^{-3}	31.05
CF_2^+	1.66E + 15 m^{-3}	5.38E + 14 m^{-3}	209.40
CF^+	7.16E + 14 m^{-3}	5.53E + 14 m^{-3}	29.60
CF	1.07E + 16 m^{-3}	7.73E + 15 m^{-3}	92.09
HF	5.19E + 16 m^{-3}	5.31E + 16 m^{-3}	2.13
HF^+	1.27E + 14 m^{-3}	1.34E + 14 m^{-3}	5.3
T_e	3.56 eV	3.60 eV	1.11
n_e	3.45E + 18 m^{-3}	3.42E + 18 m^{-3}	0.86

The 71 reaction rates that constitute the reduced 1–30 mTorr $CF_4/O_2/N_2/H_2$ are available from QDB.

Table 6 retains more of the full chemical species (25 species) when compared to table 2 which contains 21 species. This retention is a result of our method of analysis which identifies dominant reaction pathways without resorting to sweeping generalizations as in table 2. Table 2, however, does illustrate that chemistry set reduction can occur with sensible argument and knowledge of the plasma physics, and this is shown by the largest percentage change being 91.52% in H_2—which developed due to the removal of H_2 losses from the set. The largest changes in table 6 are seen to be in species with densities that are a lot smaller than the electron density, which therefore makes their participation within the chemistry set more uncertain. It can be seen, however, that the behavior of the plasma remains largely unchanged due to the near identical values of electron density and temperature—which are crucial plasma parameters.

4. Conclusions

Using 0D modeling in conjunction with validated data from QDB [7] enables the rapid study of simple to complex chemistries for process development. However, process

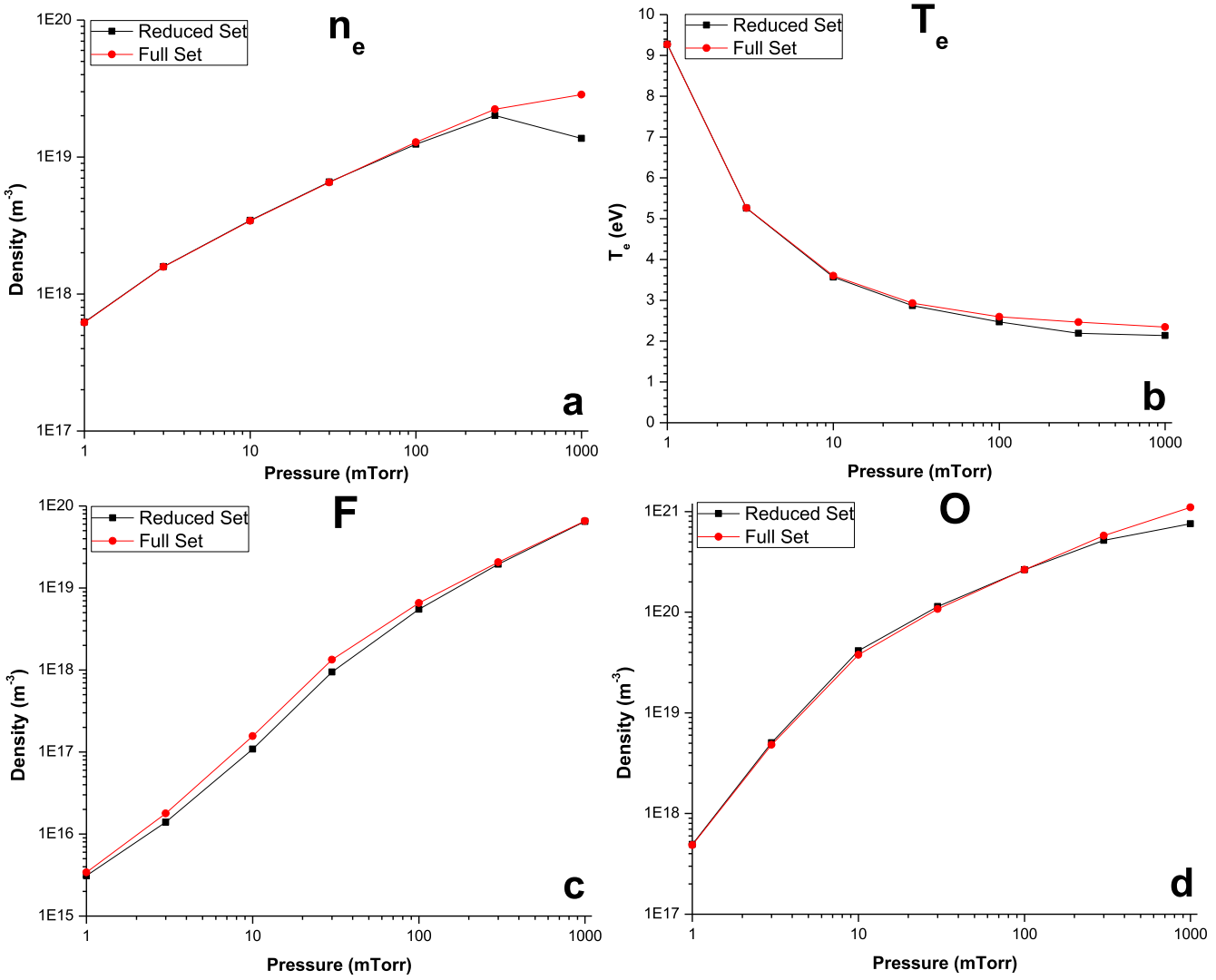

Figure 9. Comparison of various species for the full chemistry and a reduced chemistry generated for $CF_4/O_2/N_2/H_2$ at low pressure for the (a) electron density, (b) electron temperature, (c) F density, and (d) O density.

development and general innovation follows a workflow that is often constrained by the understanding and complexity of the chemistry of the species involved. We show that by considering the appropriate pressure regimes, power disposition and other general considerations, the chemistry needed for such studies can, in favorable cases, be greatly simplified. The simplified or reduced chemistries are much more suitable for reactor models performed in two or three dimensions.

Using stoichiometric sensitivity analysis as a way to reduce chemistries by determining the important reaction pathways without deviating from the physical discharge was demonstrated here. Turner [34] commented that investigating uncertainty and error to reduce complex chemistry is possible, but not the best way. A more systematic approach involving dimension reduction based upon principal component analysis is provided by Perenboom *et al* [35]. Indeed our results show that focusing on only uncertainty can become misleading, as demonstrated with the O_2 dissociation pathway. However, the method displayed here actually uses stoichiometric coefficients to evaluate production and losses. In the case of insensitive reaction pathways, these are more easily seen in a local system rather than visualizing the system as a whole. This was again seen with the O_2 DEA pathway and the increasing divergence of F^-/CF_3^+ in the $CF_4/N_2/O_2/H_2$ species when the gas pressure was increased.

Comparisons can be made with Markosyan *et al* [13] reporting the use of their PumpKin tool. Markosyn uses the example of O_3^- destruction to suggest that the reaction pathway $O_3^- + O \rightarrow O_2 + O_2 + e$ was responsible for 94% of the total O_3^- destruction. Our analysis at the high pressure regime, however, suggests that O_3^- destruction is split (52% and 42% respectively) between $O_2^+ + O_3^- \rightarrow O + O + O_3$ and $O_2^+ + O_3^- \rightarrow O_2 + O_3$. Identification of dominant pathways is therefore dependent on system pressure and power deposition in the 0D reactor. It is the current aim to improve this method for the purposes of dynamic chemistry assembling and reduction.

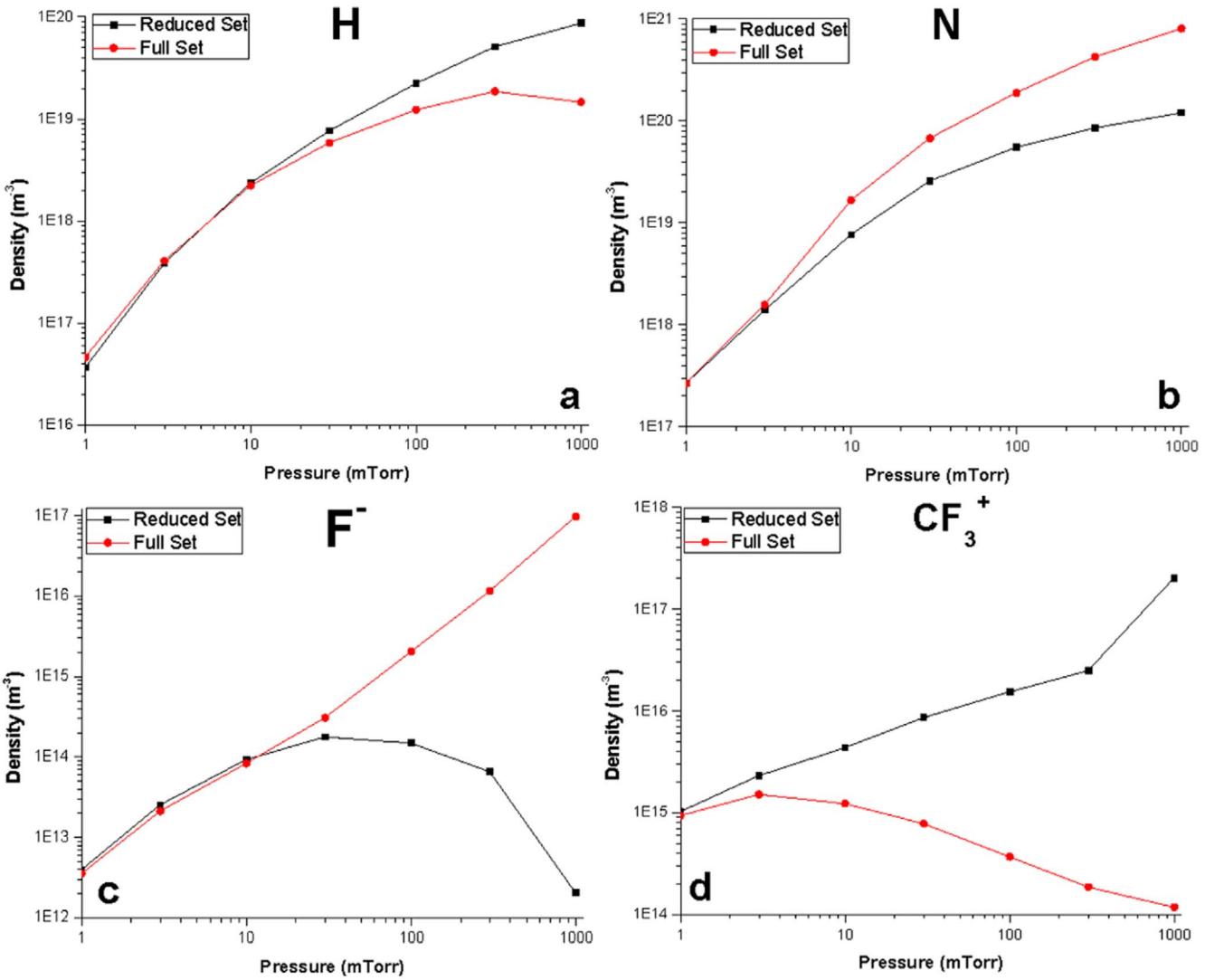

Figure 10. Comparison of various species for the full chemistry and a reduced chemistry generated for $CF_4/O_2/N_2/H_2$ at low pressure for the (a) H density, (b) N density, (c) F^- density, and (d) CF_3^+ density.

Acknowledgments

We thank Trymax for helpful discussions and sharing information about their reactor which prompted an investigation into this complex chemistry. This project received funding from the Electronic Component Systems for European Leadership Joint Undertaking under the Powerbase project, grant agreement No 662133. This Joint Undertaking receives support from the European Union's Horizon 2020 Research and Innovation Programme and Austria, Belgium, Germany, Italy, Netherlands, Norway, Slovakia, Spain, United Kingdom.

References

[1] Bartschat K and Kushner M J 2016 *Proc. Nat. Acad. Sci.* **113** 7026
[2] Adamovich I *et al* 2017 *J. Phys. D: Appl. Phys.* **50** 323001
[3] Yoon J S *et al* 2011 *AIP Conf. Proc.* **1344** 197
[4] Wakelam V *et al* 2015 *Astrophys. J. Suppl.* **217** 20
[5] Celiberto R *et al* 2016 *Plasma Sources Sci. Technol.* **25** 033004
[6] Pitchford L C *et al* 2017 *Plasma Proc. Polymers* **14** 1600098
[7] Tennyson J *et al* 2017 *Plasma Sources Sci. Technol.* **26** 055014
[8] Song M Y *et al* 2015 *J. Phys. Chem. Ref. Data* **44** 023101
[9] Song M Y *et al* 2017 *J. Phys. Chem. Ref. Data* **46** 013106
[10] Song M Y *et al* 2017 *J. Phys. Chem. Ref. Data* **46** 043104
[11] COMSOL Multiphyiscs Software, see www.comsol.com/comsol-multiphysics
[12] Holdship J *et al* 2018 *Astrophys. J.* **116** 866
[13] Markosyan A H *et al* 2014 *Comp. Phys. Comms.* **185** 2697
[14] Kokkoris M *et al* 2008 *J. Phys. D: Appl. Phys.* **41** 195211
[15] Kokkoris G *et al* 2009 *J. Phys. D: Appl. Phys.* **42** 055209
[16] Turner M M 2016 *Plasma Sources Sci. Technol.* **25** 015003
[17] Lam S H 1995 Reduced chemistry modelling and sensitivity analysis *Mechanical and Aerospace Engineering, Princeton University, Phys.* **42** 055209 (https://researchgate.net/publication/2504582_Reduced_Chemistry_Modeling_and_Sensitivity_Analysis)
[18] Fracassi F *et al* 1995 *J. Vac. Sci. Technol.* A **13** 335
[19] Matsuo P J *et al* 1997 *J. Vac. Sci. Technol.* A **15** 1801

[20] Premachandran V 1990 *Appl. Phys. Letts.* **57** 678
[21] Christophorou L G, Olthoff J K and Rao M V V S 1996 *J. Phys. Chem. Ref. Data* **25** 1341
[22] Song S H and Kushner M J 2012 *Plasma Sources Sci. Technol.* **21** 055028
[23] Hayash M 1979 *J. Phys. Colloques* **40** 661
[24] Phelps A V 1975 *Compilation of Electron Cross Sections* (unpublished)
[25] Hayashi M 1990 Electron collision cross-sections determined from beam and swarm data by Boltzmann analysis ed M Capitelli and J N Bardsley *Nonequilibrium Processes in Partially Ionized Gases* vol 1990 (New York: Springer) p 333
[26] Stief L J 1970 *J. Chem. Phys.* **52** 4841
[27] Bonham R A 1994 *Jpn. J. Appl. Phys.* **33** 4157
[28] Vasenkov A V *et al* 2004 *J. Vac. Sci. Technol.* A **22** 511
[29] Bose D *et al* 2003 *Plasma Sources Sci. Technol.* **12** 225
[30] Yang W *et al* 2018 *Plasma Sources Sci. Technol.* **27** 075006
[31] Brian J and Mitchell A 1990 *Phys. Rep.* **186** 215
[32] Itikawa Y 2009 *J. Phys. Chem. Ref. Data* **38** 1
[33] Kossyi I A *et al* 1992 *Plasma Sources Sci. Technol.* **1** 207
[34] Turner M M 2015 *Plasma Sources Sci. Technol.* **24** 035027
[35] Peerenboom K *et al* 2015 *Plasma Sources Sci. Technol.* **24** 025004